Communications in Physics, Vol. 32, No. 3 (2022), pp. 275-284
DOI: https://doi.org/10.15625/0868-3166/16541

NEAR INFRARED METAL-INSULATOR-METAL SURFACE PLASMON RESONANCES FOR REFRACTIVE INDEX SENSORS

THI HONG CAM HOANG[1,†], TUAN MINH HA[1], VAN DAI PHAM[2]
AND QUANG MINH NGO[1]

[1]*University of Science and Technology of Hanoi, Vietnam Academy of Science and Technology, 18 Hoang Quoc Viet, Cau Giay, Hanoi, Vietnam*

[2]*Institute of Materials Science, Vietnam Academy of Science and Technology, 18 Hoang Quoc Viet, Cau Giay, Hanoi, Vietnam*

E-mail: †hoang-thi-hong.cam@usth.edu.vn

Received 30 November 2021; *Accepted for publication 21 December 2021*
Published 19 May 2022

Abstract. *This work reports the optical properties of surface plasmon resonance (SPR) based on the metal-insulator-metal (MIM) structure towards a refractive index sensor. The MIM-SPR structure operating near infrared region consists of lateral periodicity of subwavelength gold patterns placed on a stack of thin silica spacer and silver film (acting as a reflector) on a silicon substrate. The reflection spectra and the electric field distributions of MIM-SPR structures can be tuned by modifying the geometrical properties and have been numerically investigated by using Lumerical's finite-difference time-domain (FDTD) solutions. The square lattice configuration of 1200 nm to 1400 nm pitch of gold micro-disks of thickness from 80 nm to 120 nm have been conducted. The size of these considered gold patterns, i.e., the diameter of the micro-disks is in the range of 900 nm to 1000 nm. The proposed MIM-SPR structure possessing sensitivity of 370 nm per refractive index unit (RIU), can be applicable for a wide variety of plasmonic sensing, in particular for refractometric biosensors.*

Keywords: surface plasmon resonance; metal-insulator-metal; refractometric biosensors.

Classification numbers: 73.20.Mf; 73.40.Rw; 87.85.fk.

I. INTRODUCTION

Surface plasmon resonance (SPR) phenomenon happens when the electric field of the light couples with the surface conduction electrons to induce collective and coherent oscillation [1]. Plasmonics, i.e. the interaction of electromagnetic radiation waves with free-charge oscillations

at the metal surface, has also achieved great attention within the photonics community. SPRs are classified into two types including surface plasmon polaritons (SPPs) or propagating surface plasmon resonance (PSPR) and localized surface plasmon resonance (LSPR) [2–5]. For LSPRs, light interacting with free electrons in the material leading to a charge separation between the electrons and the ionic metal core and in turn the Coulomb repulsion between the free electrons acting as a restoring force pushes the free electrons to move in the opposite direction [6]. For PSPRs, a metal-insulator interface supports charge density oscillations along the interface [1, 2].

Plasmonic nano/micro-structures can confine light at the subwavelength scale and thus offer novel applications in various areas of photonics. Understanding SPR has led to the development of many new plasmonic nanoparticle structures with utility in many applications including photoacoustic imaging [7, 8], photothermal cancer therapy [9], biosensor and immunoassay development [10–12], spectroscopic applications [2], and surface enhanced Raman spectroscopy (SERS) [13].

Among various kinds of SPR sensors from traditional types such as optical fiber sensors to novel ones such as racetrack resonator and metallic grating sensors [14–16], the metal-insulator-metal (MIM) configurations have been of great interest for their high absorbance efficiency [17, 18]. With the aim to target the bio-applications, sensors operate in near infrared where the fluorescent molecules emit, are of interest, because in these regions the absorption of water or other bio-materials are low. However, SPR-MIM sensors have been widely investigated using the metallic patterns of nanometers [19–21]. The sensing behavior of the SPR-MIM sensors in which employing the micro metallic pattern arrays have rarely been studied. The size of the metallic patterns is in the micrometer scale, so they can be fabricated by physical methods which are less sophisticated than those used for nanometer size metallic patterns.

In here, the optical properties and PSPR sensing ability of MIM noble metal periodic array structures in the near infrared wavelength range have been numerically studied using numerical electromagnetic simulation, i.e., the finite difference time domain (FDTD) by Lumerical's FDTD solutions [22], with the aim to exploit both the MIM configuration which helps confine the light and the benefit of periodicity to transfer the incident energy to SPPs. The size of the metallic patterns is in the micrometer scale, so they can be easily fabricated by physical methods such as direct laser writing. In our work, the reflection spectra and electric field distribution of gold periodic micro-disk arrays in square lattice placed on a stack of thin silica spacer and silver film on a silicon substrate have been considered with taking into account the effect of geometrical parameters of said structures: diameter D, lattice constant P and gold thickness H in order to elucidate the relationship between the plasmonic properties and these structural features. Then the suitable structure for refractive index sensing. The shift of resonance dips when considering different refractive index cladding has been monitored and the sensitivity of the optimized gold micro-disk array of 370 nm/RIU has been reported, which is in the same scale with the sensitivity obtained by other gold nano-structured configurations.

II. SIMULATIONS

Figure 1 (a) shows the typical geometry, consisting of an MIM made of gold micro-disk arrays, simulated by the 3D Lumerical's FDTD solutions. A 100 nm thick Ag layer was introduced onto a silicon substrate, as a reflector in order to prevent the light from transmitting into the silicon substrate. A 40 nm silica (SiO_2) layer was then coated on to the Ag layer and an array

of gold micro-disks is deposited on to the silica spacer in the square lattice. The silica layer as a spacer separating the micro-disk arrays and the Ag film, was used to induce strong coupling between the surface plasmons localized in each disk and the propagating surface plasmons in the disk array. The size of the MIM-SPR structure is directly correlated with the optical properties, therefore in here we study the optical behaviors of the structure under the change of the geometrical parameters, i.e., the diameter and the lattice constant of gold micro-disk array, the thickness of the gold micro-disk. Throughout this work, the typical values of the structure are as follows, the diameter of the gold micro-disk is D =950 nm, the lattice constant P=1300 nm and the thickness of gold is H=100 nm. These geometrical parameters are selected so that the MIM-SPR structure operates in the near-infrared wavelength, i.e., from 1200 nm to 1800 nm. Starting from these reference values, the effect of the geometrical parameters on the optical behaviors of the structure are then considered. A gold micro-disk periodic array thickness ranging from 80 nm to 120 nm is under investigation. The gold pattern diameter varies from 900 nm to 1000 nm. These gold micro-disk patterns are distributed in a square lattice with the value of lattice constant changes from 1200 nm to 1400 nm. The optical properties of this structure including the reflection spectra and the electric field distribution have been realized by using Lumerical's FDTD solutions.

Figure 1(b) illustrates one gold unit cell containing a gold micro-disk in a square lattice and the simulation monitors defined in Lumerical's FDTD solutions. In which the reflection spectra and the electric field profile are collected by the reflection monitor and the electric field monitor. The light source injecting the TEM signal in z -direction and the monitors collecting reflection spectra and electric field distribution at the metal region are arranged in perspective view and side view as depicted in Fig. 1(b) and (c), respectively. In the simulation, the periodic boundaries in x and y direction are chosen while perfectly matched layer absorbing boundary conditions are used at the upper and lower boundaries in order to generate the planar periodic structures. The effect of different geometrical parameters, i.e., the diameter of gold micro-disk, the lattice constant and the gold thickness on the optical characteristics of the MIM-SPR structures have been investigated starting from the set of geometrical values mentioned above. In all simulations, the reference structure is kept unchanged and only one parameter (diameter, lattice constant or thickness) is varied with aim to study how the optical properties and electric field distribution would behave depending on that parameter. Then the most suitable structure for further study the refractive index sensing property of the micro-disk array is thus derived.

III. RESULTS AND DISCUSSION

III.1. Effect of gold pattern diameter

Figure 2 shows the reflection spectra of the MIM-SPR periodic array structure of the gold micro-disk when increasing the diameter D from 900 nm (red circle symbol) to 950 nm (black solid line) and 1000 nm (blue dashed line) while considering the lattice constant of 1300 nm, the gold thickness of 100 nm. It is noticed that there are two modes in the 1200 nm -1800 nm wavelength range, namely the first mode (longer wavelength) and second mode (shorter wavelength), denoted by mode 1 and mode 2 in the figure. The resonances correspond to the dips in the reflection spectra. In this configuration, the resonances can be resulted from following phenomena: the incident energy is coupled to the surface plasmon wave localized via the single gold micro-disk and the incident energy is also transferred to PSP through the periodic array. As seen from the

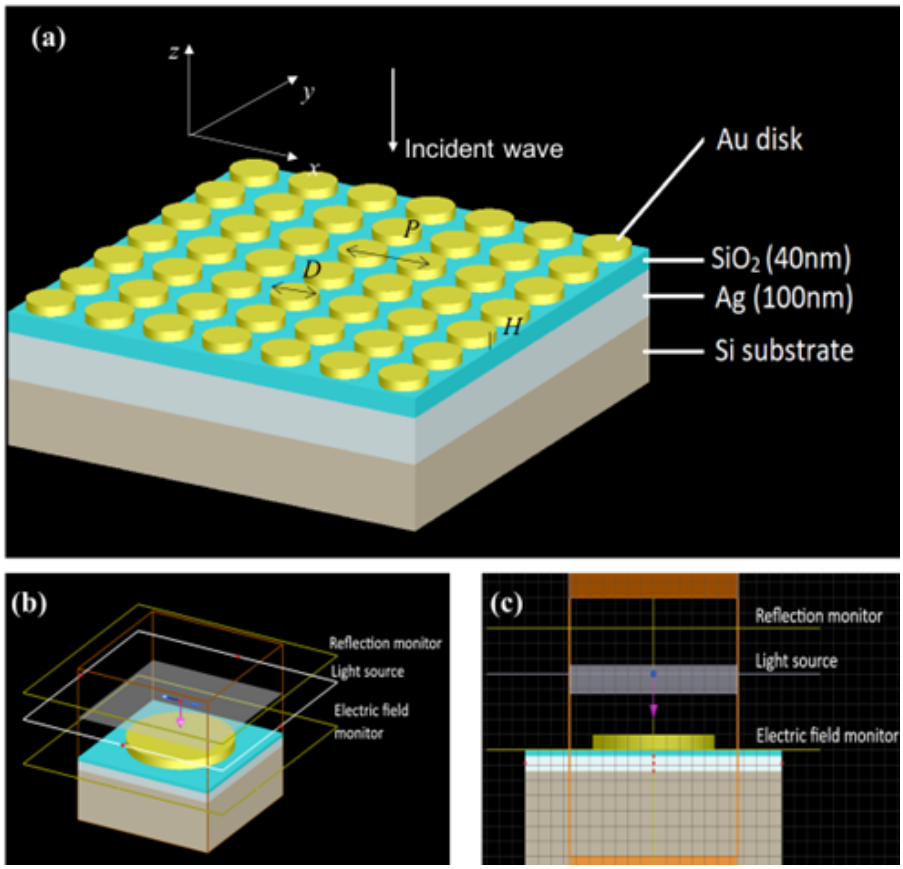

Fig. 1. (a) Gold micro-disk array structure under (b) FDTD simulation in perspective view and (c) FDTD in side-view of the MIM-SPR structure.

electric field distribution in the side view shown in Fig. 2, the SPPs clearly exist and the electric field enhancement in these modes corresponds to the strong coupling between the LSP and PSP. From the electric field profile at the gold-silica interface, it is shown that the electric field of the first mode distributes radially in the edge of the surface as well as in the interface between the gold unit and the silica layer. Besides, the electric field of the second mode is localized symmetrically inside the gold unit. They are similar to the longitudinal plasmonic band (LPB) and the transverse plasmonic band (TPB) as discussed in [23] based on the direction of the electron oscillation inside the gold nano-rods. The occurrence of these two modes is due to the specific geometry of the gold microdisk structures, which also happen for gold nanorods [24, 25], nanowires [26], nanodisks [5, 23] and cylinders [27] as these typical geometries usually induce two main circulation paths, one corresponding to the transverse and the other to the longitudinal SPR modes.

Furthermore, the intensity of these two resonances modulates in different fashion as depicted in Fig. 2. The TBP is much weaker in intensity than the LTP as noticed in gold nanorods [28]. For the case of the transverse mode, the intensity of the mode remains more or less the same while there is a significant change in the intensity due to the influence of the gold diameter increase.

The electric field of the gold micro-disk at the gold-silica interface of the first mode is distributed radially on the circle in the micro-disk due to the circular symmetry of the structure, hence the intensity of this mode is dramatically changed by the size of the micro-disk. It is evidenced that with increasing the diameter *D,* the intensity of the peaks decreases, which is also reported in other works [26, 29].

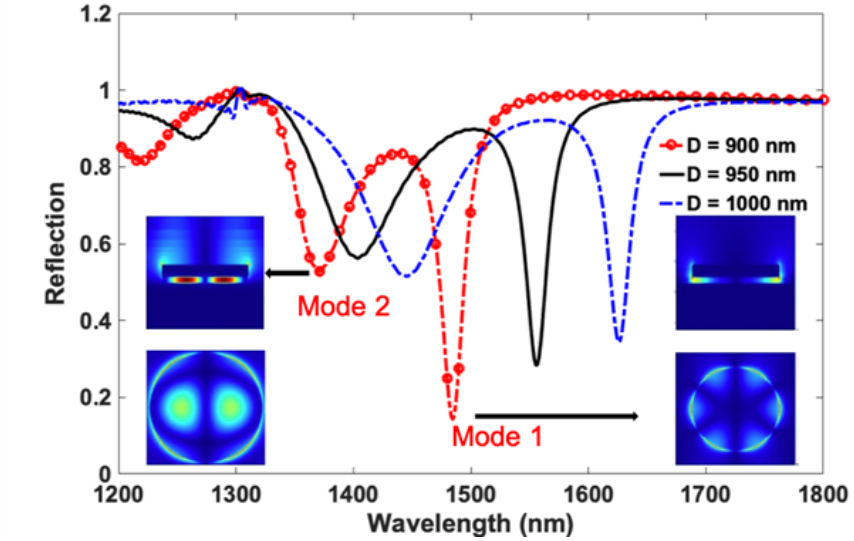

Fig. 2. (color online) (a) Reflection spectra of the MIM-SPR periodic array structure when increasing the diameter D of gold micro-disk from 900 nm (red circle symbol) to 950 nm (black solid line) and 1000 nm (blue dashed line), the lattice constant $P =$ 1300 nm and gold thickness $H = 100$ nm; insets: the side view and top view at the gold-silica interface of the electric profile corresponding to two resonances.

It is also observed that the resonance wavelength red-shifts as the size of the gold pattern increases, and the peak distance gets larger while the intensity drop is less significant. This redshift of the resonant modes of the structures towards lower frequencies is attributed to the increase of the effective index of the guiding layer when the size of gold micro-disk is enlarged [30]. In addition, from the electric field distribution of the two resonant modes, the second mode of gold micro-disk has been found to be insensitive to the changes in the size of the gold micro-disk and also this mode has been shown to be insensitive to and the surrounding refractive index, whereas the first mode shows a red-shift with the increase of size of gold micro-disk and this is very sensitive to any change of the refractive index as reported in other researches [24, 30, 31]. Therefore, the first mode has advantages in refractive index sensing applications.

III.2. Effect of lattice constant

The optical characteristics of the MIM-SPR structures under the change of the lattice constant are shown in Fig. 3. The reflection spectra and the electric profile of the structures when the lattice constant changed from 1200 nm (red circle symbol) to 1300 nm (black solid line) and

1400 nm (blue dashed line) while the gold diameter is maintained at 950 nm and the thickness of gold layer is of 100 nm are depicted.

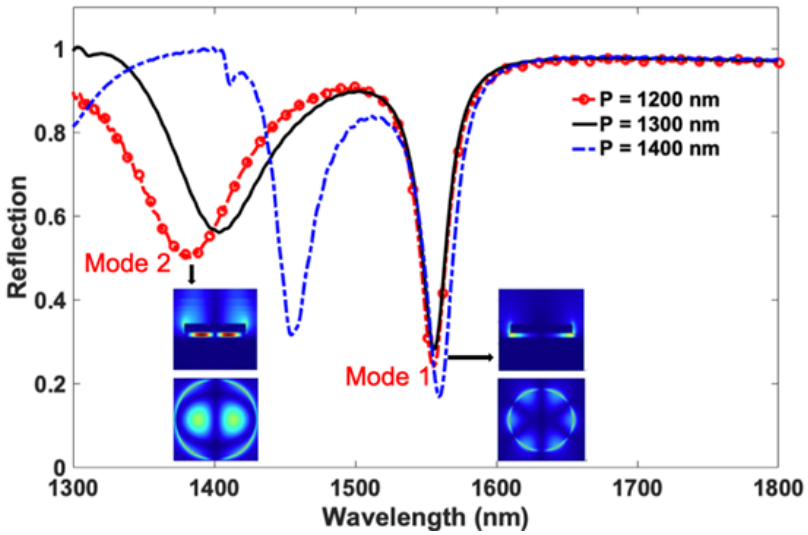

Fig. 3. (a) Reflection spectra of the MIM-SPR periodic gold micro-disk array structures when the lattice constant P is changed from 1200 nm (red circle symbol) to 1300 nm (black solid line) and 1400 nm (blue dashed line), the gold diameter D = 950 nm and the thickness of gold layer H=100 nm; insets: the side view and top view at the gold-silica interface of the electric profile corresponding to two resonances.

In here, as the lattice constant increases, mode 2 (shorter wavelength) is red-shifted while mode 1 (longer wavelength) remains unchanged. This response may cause mode 2 interact with mode 1 if the lattice constant keeps increasing. Moreover, if the value of the period is too large, the structure does not exhibit the advantages for the plasmonic sensors due to the anti-crossing behavior [19].

III.3. Effect of gold thickness

Figure 4 presents the reflection spectra of the MIM-SPR periodic array structure of the gold micro-disk when increasing the gold thickness of the micro-disk structure from 80 nm to 120 nm. It is seen that the resonant intensity and the resonance wavelength changes when the gold layer gets thicker from 80 nm to 120 nm with a 20 nm step. Increasing the thickness of gold micro-disks results in a noticeable change in intensity, as the mode 1 exhibits a lower intensity drops, and in contrast the intensity of the second mode becomes weaker. In addition, the increase of thickness of gold layer generates a significant red-shift of the second mode while the resonant wavelength of the first mode is affected negligibly. The behaviour of these two resonant modes can be explained by the fact that the first sharp dip at longer wavelength corresponds to a surface plasmon wave localized in the gold micro-disks while the second shallow dip is resulted from the periodic arrays. Thus, the first mode is dramatically affected by changes in gold pattern diameter and is slightly affected by the periodicity as well as the gold pattern thickness. In a manner similar

to the influence of the lattice constant, mode 2 may get closer and interact with mode 1 if the gold layer becomes thicker.

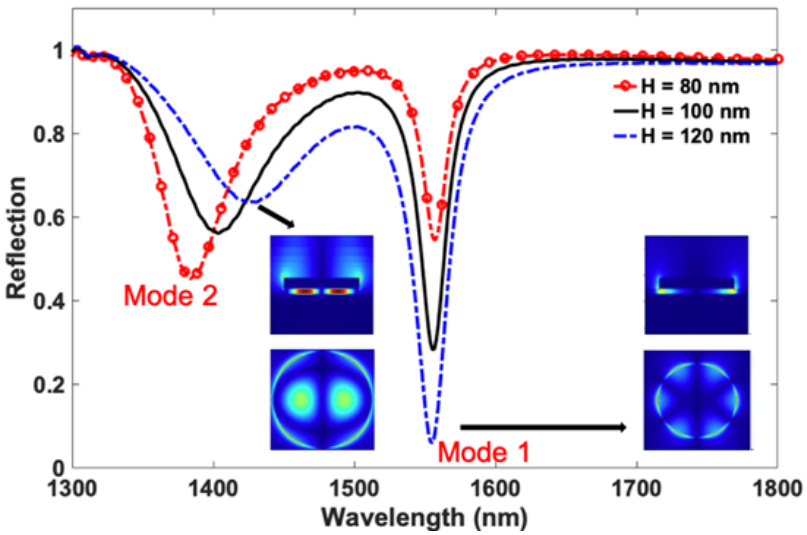

Fig. 4. Reflection spectra of the MIM-SPR periodic array structure of the micro-disk when increasing the gold thickness H from 80 nm (red circle symbol) to 100 nm (black solid line) and 120 nm (blue dashed line) and the gold diameter D =950 nm, the lattice constant P=1300 nm; insets: the side view and top view of the electric profile corresponding to two resonances.

III.4. Refractive index sensing applications

Regarding sensing application, the change of the vicinity environment refractive index on top of the gold micro-disk arrays causes a resonant peak shift, thus the medium refractive index can be sensed by detecting the position of the resonant peak. In order to evaluate the quality of a reflective index sensor, the sensitivity (S) is typically utilized. For plasmonic sensors, the sensitivity is commonly defined in terms of the change or shift of a measurable parameter, typically the resonant wavelength, for detection of refractive index [17]. The refractive index sensitivity is defined as $S = \Delta\lambda/\Delta n$ where $\Delta\lambda$ is the shift of the resonant peak wavelength and Δn is the refractive index change of the analyte. As a great performance refractive index sensor should possess high sensitivity, therefore the dip depth should be small. In this spirit, the structure possesses large peak distance and the reflection intensity at resonance reaches close to zero is awaited. For that purpose, the first mode of the gold micro-disk with high respect ratio ($H = 120$ nm) is of interest because of its narrow spectral linewidth while the second mode is insufficient for refractive index sensing due to its small resonant intensity in comparison with the other, as discussed in the previous sections. Considering the change in lattice constant, a lower value is preferred due to better peak separation, however in order to avoid signal noise, P= 1300 nm is chosen over P=1200 nm. Under the influence of the diameter, peak separation is prioritized, but also intensity of the first mode should be sufficient, therefore the mid-point value D=950 nm is selected. Henceforth, the

gold micro-disk periodic array set of parameter $D = 950$ nm, $P = 1300$ nm, and $H = 120$ nm is adopted for refractive index sensing in the near infrared wavelength range from 1550 nm to 1670 nm.

The reflection spectra of the above structure with different cladding material refractive index are illustrated in Fig. 5(a) to demonstrate the influence of the cladding material on the resonant mode. It is crystal clear that the resonant peaks show red shifts as the refractive index increases, while the linewidth and the intensity of these spectra are almost the same. The reason is that when the refractive index of the cladding material changes a small amount, the property of the surface plasmon mode in the structure is not significantly affected. The top view and the side view of electric field distribution of the first mode are shown in the inset of Fig. 5(a) and remain for these five resonances (mode 1).

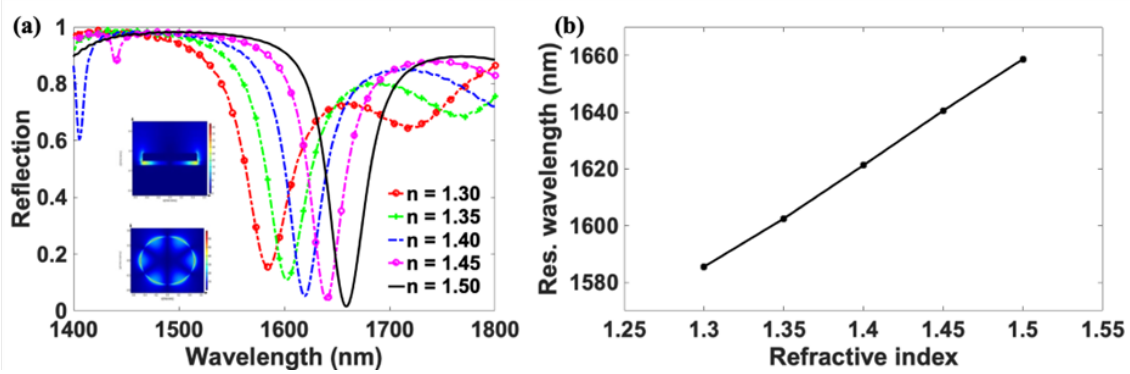

Fig. 5. (a) The dependence of the reflection spectra on the cladding material, the refractive index changes from 1.3 to 1.5; insets: the top view and side view of the electric field profile at resonance of the mode 1; (b) The position of the resonant wavelength (mode 1) as a function of the refractive index. The values of the gold micro-disk arrays in the MIM-SPR structure here are parameter $D = 950$ nm, $P = 1300$ nm, and $H = 120$ nm.

Figure 5(b) describes a good linear relationship between the position mode 1 and the refractive index of the cladding material. The resonance redshifts linearly as the refractive index of the cladding material increases and the sensitivity is the change of wavelength over the change of the refractive index and is calculated to be 370 nm/RIU. This obtained sensitivity in our proposed MIM gold-micro disk array can be comparable with the sensitivity achieved in other gold nano-structured configurations [20, 21].

IV. CONCLUSION

In this work, the optical properties of gold periodic arrays onto a thin stack of silica spacer and a silver layer deposited onto a silicon substrate have been investigated in the infra-red range. Using Lumerical's FDTD solutions, the influence of the geometrical properties on the reflection spectra and the electric field distributions of these MIM-SPR structures have been investigated. With a 950 nm diameter and 1300 nm lattice constant for the gold micro-disk array of 120 nm height, the achieved sensitivity of the micro-disk MIM-SPR structure to be of 370 nm/RIU. The

obtained result shows the possibility of the proposed structure to behave as a potential candidate for biological sensors.

ACKNOWLEDGMENTS

This research is funded by Vietnam National Foundation for Science and Technology Development (NAFOSTED) under grant number 103.03-2020.04.

REFERENCES

[1] S. A. Maier, *Plasmonics: Fundamentals and Applications*, Springer, USA, 2007.
[2] J. Jatschka, A. Dathe, A. Csáki, W. Fritzsche, and O. Stranik, *Propagating and localized surface plasmon resonance sensing - a critical comparison based on measurements and theory*, *Biosens. Bioelectron.* **7** (2016) 62.
[3] J. Jana, M. Ganguly, and T. Pal, *Enlightening surface plasmon resonance effect of metal nanoparticles for practical spectroscopic application*, *RSC Adv.* **6** (2016) 86174.
[4] M. S. Nezami and E. Gordon, *Localized and propagating surface plasmon resonances in aperture-based third harmonic generation*, *Opt. Express* **23** (2015) 251035.
[5] Q. Ma, Q. Liu, S. Feng, Y. Chen, and W. Cai, *Interaction properties between different modes of localized and propagating surface plasmons in a dimer nanoparticle array*, *Opt. Eng.* **57** (2018) 087108.
[6] E. Petryayeva and U. Krull, *Localized surface plasmon resonance: Nanostructures, bioassays and biosensing-A review*, *Anal. Chim. Acta* **706** (2011) 8.
[7] Y. Mantri and J. V. Jokerst, *Engineering Plasmonic Nanoparticles for Enhanced Photoacoustic Imaging*, *ACS Nano* **14** (2020) 9408.
[8] C. L. Bayer, S. Y. Nam, Y-S. Chen and S. Y. Emelianov, *Photoacoustic signal amplification through plasmonic nanoparticle aggregation*, *J. Biomed. Opt.* **18** (2013) 016001.
[9] K. Turcheniuk, T. Dumych, R. Bilyy, V. Turcheniuk, J. Bouckaert, V. Vovk, V. Chopyak, V. Zaitsev, P. Mariot, N. Prevarskaya, R. Boukherroub, and S. Szunerits, *Plasmonic photothermal cancer therapy with gold nanorods/reduced graphene oxide core/shell nanocomposites*, *RSC Adv.* **6** (2016) 1600.
[10] J. S. Seok and H. Ju, *Plasmonic optical biosensors for detecting C-reactive protein: A review*, *Micromachines* **11** (2020) 0895.
[11] N. Kongsuwan, X. Xiong, P. Bai, J.-B. You, C. E. Png, L. Wu, and O. Hess, *Quantum Plasmonic Immunoassay Sensing*, *Nano Lett.* **19** (2019) 5853.
[12] A. M. Shrivastav, U. Cvelbar, and I. Abdulhalim, *A comprehensive review on plasmonic-based biosensors used in viral diagnostics*, *Commun. Biol.* **4** 70 (2021).
[13] T. B. Pham, T. H. C. Hoang, V. H Pham, V. C. Nguyen, T. V. Nguyen, D. C. Vu, V. H. Pham, and H. Bui, *Detection of permethrin pesticide using silver nano-dendrites SERS on optical fibre fabricated by laser-assisted photochemical method*, *Sci. Rep.* **9** (2019) 12590.
[14] A. K. Sharma, R. Jha, and B. D. Gupta, *Fiber-Optic sensors based on surface plasmon resonance: A comprehensive review*, *IEEE Sens. J.* **7** (2007) 1118.
[15] X. Wang, H. Jiang, J. Chen, P. Wang, Yo. Lu, and H. Ming, *Optical bistability effect in plasmonic racetrack resonator with high extinction ratio*, *Opt. Express* **19** (2011) 19415.
[16] Y. Chen and H. Ming, *Review of surface plasmon resonance and localized surface plasmon resonance sensor*, *Photonic Sens.* **2** (2012) 37.
[17] G. Li, X. Chen, O. Li, C. Shao, Y. Jiang, L. Huang, B. Ni, W. Hu, and Wei Lu, *A novel plasmonic resonance sensor based on an infrared perfect absorber*, *J. Phys. D: Appl. Phys.* **45** (2012) 205102.
[18] C-Y. Chang, H-T. Lin, M-S Lai, T-Y Shieh, C-C Peng, M-H Shih, and Y-C Tung, *Flexible localized surface plasmon resonance sensor with Metal- Insulator-Metal nanodisks on PDMS substrate*, *Sci. Rep.* **8** (2018) 11812.
[19] Y. Chu and K. B. Crozier, *Experimental study of the interaction between localized and propagating surface plasmons*, *Opt. Lett.* **34** (2009) 244.
[20] Z. Zhang, L. Wang, H. Hu H, K. Li, X. Ma, and G. Song, *A high figure of merit localized surface plasmon sensor based on a gold nanograting on the top of a gold planar film*, *Chin. Phys. B* **22** (2013) 104213.

[21] S. Wang, X. Sun, M. Ding, G. Peng, Y. Qi, Y. Wang and J. Ren, *The investigation of an LSPR refractive index sensor based on periodic gold nanorings array*, *J. Phys. D: Appl. Phys.* **51** (2018) 045101.
[22] https://www.lumerical.com/products/fdtd/, Fri. 10 Sep. 2021.
[23] K. Imura, K. Ueno, H. Misawa, H. Okamoto, D. McArthur, B. Hourahine, and F. Papoff, *Plasmon modes in single gold nanodiscs*, *Opt. Express* **22** (2014) 12189.
[24] J. Cao, T. Sun and K.T.V. Grattan, *Gold nanorod-based localized surface plasmon resonance biosensors: a review*, *Sens. Actuators B Chem.* **195** (2014) 332.
[25] N. A. Bang, P. T. Thom, and H. N. Nhat, *A comparative study of classical approaches to surface plasmon resonance of colloidal gold nanorods*, *Gold Bull.* **46** (2013) 91.
[26] I. Alber, W. Sigle, Sv. Muller, R. Neumann, O. Picht, M. Rauber, P. A. van Aken, and M. E. Toimil-Molares, *Visualization of multipolar longitudinal and transversal surface plasmon modes in nanowire dimers*, *ACS Nano* **12** (2011) 9845.
[27] S. Belan and S. Vergeles, *Plasmon mode propagation in array of closely spaced metallic cylinders*, *Opt. Mater. Express* **5** (2015) 130.
[28] L. Ma, S. Liang, X-L. Liu, D-J. Yang, L. Zhou, and Q-Q. Wang, *Synthesis of dumbbell-like gold-metal sulfide core-shell nanorods with largely enhanced transverse plasmon resonance in visible region and efficiently improved photocatalytic activity*, *Adv. Funct. Mater* **25** (2014) 898.
[29] O. Nicoletti, M. Wubs, N. A. Mortensen, W. Sigle, P. A. van Aken, and P. A. Midgley, *Surface plasmon modes of a single silver nanorod: An electron energy loss study*, *Opt. Express* **19** (2011) 15371.
[30] S. Hou, X. Hu, T. Wen, W. Liu, and X. Wu, *Core-shell noble metal nanostructures templated by gold nanorods*, *Adv. Mater.* **25** (2013) 3857.
[31] Q. Ruan, C. Fang, R. Jiang, H. Jia, Y. Lai, J. Wang, and H-Q. Linc, *Highly enhanced transverse plasmon resonance and tunable double Fano resonances in gold@titania nanorods*, *Nanoscale* **8** (2016) 6514.